Nigerian Journal of Theoretical and Environmental Physics (NJTEP)
ISSN Online: 1597-9849
ISSN Print: 3026-9601
DOI: https://doi.org/10.62292/njtep.v3i1.2025.72
Volume 3(1), March 2025

The Impact of Pressure on the Structural, Electronic, and Mechanical Properties of TiPdSn: An Ab Initio Study

***[1]Ighakpata Fidelia Chukwudumebi and [2]Aigbekaen Eddy Enorense**

[1]Department of Physics, College of Education, Warri, Delta State.
[2]Department of Physics, Igbinedion University, Okada, Benin City, Nigeria

[*]Corresponding author's email: fighrakpata@yahoo.com

Keywords:
Half-Heusler,
Band gap,
Bulk modulus,
Semiconductor,
Dielectric function,
Refractive index.

ABSTRACT

The TiPdSn half-Heusler alloy structural, electronic, mechanical, and optical properties were investigated from first-principles calculations in addition to their various pressures. The projected augmented wave (PAW) type of pseudopotential within the generalized gradient approximation (GGA) was employed during the calculations. The acquired results disclosed that TiPdSn is a semiconductor with an indirect band gap. Additionally, the effect from the mechanical property revealed that TiPdSn is ductile and mechanically stable. Optical properties unveil that TiPdSn have static dielectric function of 19.42 and 24.59 at 0GPa and 150GPa respectively and the refractive index are 5.11 and 4.30 at the pressures of 0GPa and 150GPa.

INTRODUCTION

Researchers have shown significant interest in Half-Heusler alloys due to their diverse features that have practical applications in several technological industries (Zilber *et al*., 2019; Kocak and Ciftci, 2018; Babalola and Iyorzor, 2019; Inomata *et al*., 2003; Iyorzor *et al*., 2018). Half-Heusler alloys are a subset of Heusler alloys, which encompass full-Heusler alloys, quaternary Heusler alloys, half-Heusler alloys, and binary Heusler alloys. The full-Heusler alloys are typically denoted by the formula X2YZ, whereas the half-Heusler alloys are denoted by the formula XYZ. The diverse properties exhibited by these alloys make them highly valuable for various applications, including as semiconductors, thermoelectric materials, superconductors, topological insulators, magneto-optical devices, half metals, shape memory alloys, and materials with heavy-Fermion behavior (Babalola and Iyorzor, 2021; Iyorzor *et al*., 2018; Goll et al., 2008). Due to their little lattice misfit, half-Heusler alloys may be formed epitaxially a top semiconductor, making them suitable for use as spin injection devices (Okunzuwa and Aigbekaen, 2021; Aigbekaen and Ighrakpata, 2022; Aigbekaen *et al*., 2023; Chadov *et al*., 2010).

The Heusler alloy family exhibits a remarkable characteristic whereby their properties may be accurately anticipated only based on the knowledge of the quantity of valence electrons they possess. For example, half-Heusler alloys with 18 valence electrons are recognized for their semiconducting and thermoelectric properties. Half-Heusler alloys with valences below or over 18 typically exhibit ferromagnetic behavior and some of them also display half-metallic properties (Babalola *et al*., 2019; Webster *et al*., 1984; Canfield *et al*., 1991). TiPdsn is an example of 18 valence electron with semiconducting behavior and various of its features have been explored. Kaur in 2017 examined the electrical, lattice dynamics and thermoelectric characteristics of TiPdSn (Oogane *et al*., 2006). He observed that TiPdSn is an indirect semiconductor and examined the electrical, mechanical and thermoelectric properties of TiPdSn (Gautier *et al*., 2015). Zheng *et al*., 2020, have explored how the thermoelectric behavior of TiPdSn is altered when doped with Zr (Khandy and Chai, 2021). They found out that Ti0.5Zr0.5PdSn had a high figure of merit of 2.43. Gautier and his colleagues tested a variety of 18 valence electron half Heusler alloys and found out that TiPdSn is a stable half Heusler alloy (Damewood *et al*., 2015).

The optical property of TiPdSn is sparse in literature and the requirement to know the behavior of TiPdSn with light is highly invaluable in opto-electronic sector. Half-Heusler alloys also form in hexagonal crystal structure with space group P63/mmc No. 194 and P63mc No. 186. Structural phase shift from cubic phase to hexagonal phase under pressure has been described experimentally (Kaur, 2017). and theoretically (Sarker

et al., 2021) by researchers. In this study, inquiry is carried out on the structural properties of TiPdSn of the Cubic phase under various pressures. The influence of pressure was also carried out on the electrical and mechanical properties of TiPdSn.

MATERIALS AND METHODS

Computational detail

The density functional theory (DFT) is the basis of the first principles calculation performed in this study. The exchange-correlation was taken care of by employing the generalized gradient approximation and the projector augmented wave (PAW) kind of pseudopotential as developed in Quantum espresso code was used (Khandy and Gupta, 2017; Giannozzi *et al*., 2017). Before any property is computed, it is vital to adjust certain parameters which are crucial for achieving the lowest ground state energy of thecompound. These parameters include the Kinetic energy cut off, the kpoint and the lattice constants. The kinetic energy cut off of 65Ry and a kpoint of 8X8X8 were used throughout the computation with a convergence threshold of 10^{-6} eV for better results. As for the lattice constant, the total energy vs the lattice constant graph was fitted to a Birch Murnaghan equation of state in order to obtain the optimum value. Mechanical and optical characteristics were estimated using the Thermo_pw algorithm (Zheng *et al*., 2020).

RESULTS AND DISCUSSION

Structural properties

Half-Heusler alloys are face centered cubic structure having space group F-43m with no. 216. As depicted in Fig. la. Where Ti, Pd, Sn atoms are at the position of 4c (0.5, 0.5, 0.5), 4b (0.25, 0.25, 0.25) and 4a (0, 0, 0) in Wyckoff coordinates, respectively.

The structural properties of TiPdSn in the cubic phase are shown in Table 1. Results from this investigation are in good conform to other results from literature. A graph of the total energy versus the volume of the cubic phase is shown in Fig. 2. These results can be easily seen from Fig. 3. Table 2 shows the impact of pressure on the lattice constant of TiPdSn in cubic phase as well as the link length between two atoms. It is noted that these values decrease as the pressure increases.

Table 1: The Structural properties: a(Å), B(GPa), band gap near Fermi energy E_g (eV) and bond length B_L (Å) (within pressure range (0GPa and 150GPa)

	0 GPa	10 GPa	20 GPa	30 GPa	50 GPa	75 GPa	100 GPa	150 GPa
A	11.7530	11.4824	11.2772	11.1111	10.8521	10.6097	10.4188	10.1253
B	120.136	158.38	194.480	228.246	292.429	366.792	436.953	571.458
Eg	0.4694	0.5146	0.5499	0.5802	0.6263	0.6705	0.7028	0.7497
B_L	1.5548	1.5190	1.4919	1.4699	1.4357	1.4036	1.3784	1.3395

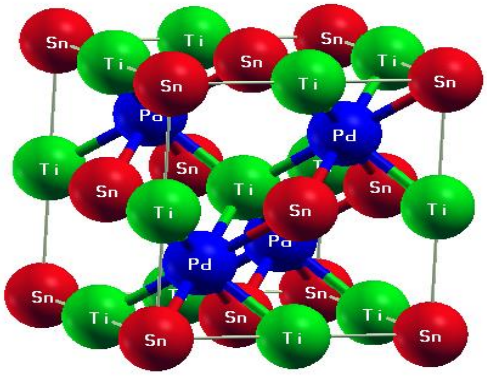

Figure 1: Crystal structure of TiPdSn HH alloys

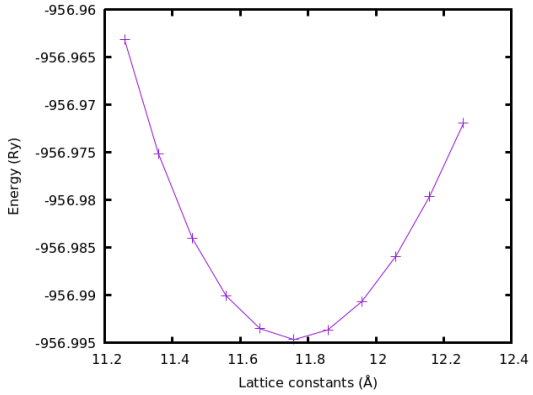

Figure 2: Energy versus Lattice constant for TiPdSn

Table 2: Lattice parameter a, bulk modulus (B), pressure derivative (B') and energy band gap Eg of TiPdSn at zero pressure

Compounds TiPdSn	Method	a(Å)	B(GPa)
Cubic	Present work Others[17]	6.22	118.7
	Others[19]	6.17	4.62
		6.23	131.21

Mechanical Properties

The characteristics of the mechanical property of TiPdSn is described in this part associated with mechanical property at 0 GPa, 10 GPa, 20GPa, 30GPa, 50 GPa, 75GPa and 100 GPa pressure are described in Table 3. The parameters that form the mechanical property of a material comprises of the elastic constants C_{ij}, the bulk, shear and Young modulus as well as the Poisson's ratio, the anisotropy and the B/G ratio. The mechanical property gives information about the rection of the materials to external forces; it also helps to ascertain if the materials are mechanically stable. The criterion for mechanical stability in cubic phase is given in equation 1

$C_{11}>0$, and $C_{44}>0$, $C_{11}>B>C_{12}$ and $C_{11}+2C_{12}>0$, $C_{11}-C_{12}>0$ (1)

From the stability stipulations, it is ascertained that TiPdSn is mechanically stable at zero pressure. From the B/G ratio, it is noticed that TiPdSn is ductile in character.

At higher pressures, the mechanical property has also been determined and is depicted in Figs. 4-7. It is observed that the elastic constants increase as pressure increases as well other parameters like the moduli, the B/G ratio and the Poisson ratio glow with rising pressure.

Table 3: Mechanical properties with C_{11}, C_{12} and C_{44} as elastic constants, Young modulus E, shear modulus G, anisotropy A, B/G ratio and the Poisson's ratio v of TiPdSn. Results in parenthesis are from (Gautier *et al*., 2015; Dal Corso, 2016; Khenata *et al*., 2006)

Compound	TiPdSn
C_{11} (GPa)	169.48(184.96)
C_{12} (GPa)	95.47(105.27)
C_{44} (GPa)	58.83(58.97)
E(GPa)	100.66(134.11)
G(GPa)	37.00
B/G	3.247
A	1.538
v	0.360(0.330)

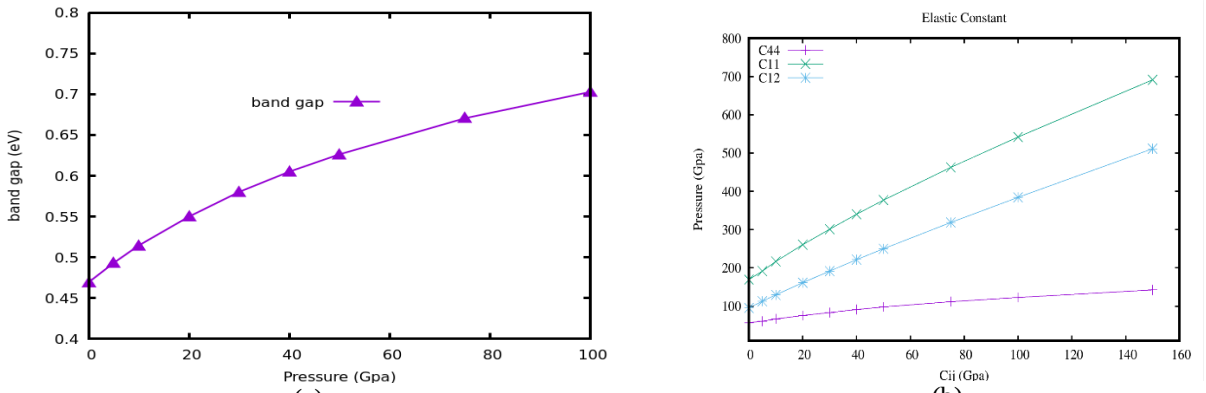

(a) (b)

Figure 3: (a) band gap vs pressure, (b) pressure vs elastic constants

Electronic Properties

The electronic band structure and density of states (DOS) for the electronic property of TiPdSn has been explored. The effect of hydrostatic pressure on the electronic property is further disclosed.

Figure 6 displayed that the half-Heusler alloy is a semiconductor with an indirect band gap of 0.5 eV. The input of each atomic orbit is realized in the DOS (Noda *et al*., 1979; Gu, J.B., Wang *et al*., 2015; Babalola *et al*., 2023).

Figure 8(a-b) are the DOS of TiPdSn at the pressure of 10GPa and 50GPa respectively. The band gap performance with respect to pressure is observed in Fig. 5(a-b) i.e. at a pressure of 10GPa, the band gap is 0.5eV and at 50GPa, the band gap is 0.6eV.

In Figure 9, at 0 GPa, inside the conduction band, the main contribution commenced from Pd-3d orbital and small from Sn-2p orbital. Their influence is far from the about 0.6eV. In the same way, the highest contribution in the valence band, the three orbitals formed their separate contributions, with Pd-3d orbital having the highest contribution and the least from Sn-2p orbital. Same is applicable in the case of 50GPa.

Vibrational properties

To investigate the vibrational properties of TiPdSn compound, the phonon spectra of diverse pressures (10GPa and 50GPa) were determined. We employ the Quantum ESPRESSO software to compute the physical properties of the materials.

Fig. 6(a-b) displays the phonon dispersion curves along the $\Gamma \rightarrow X \rightarrow W \rightarrow K \rightarrow \Gamma \rightarrow L$ high symmetry directions.

There was no negative frequencies in the compounds Brillouin zone, showing that it is dynamically stable.

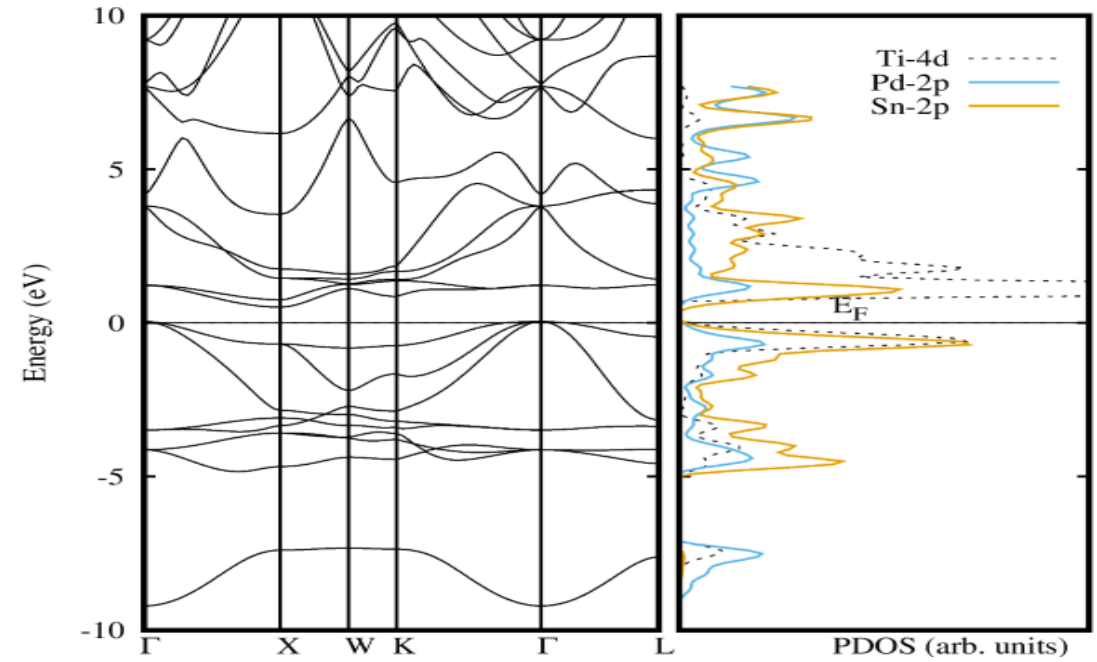

Figure 4: Electronic band structure and partial density of state TiPdSn

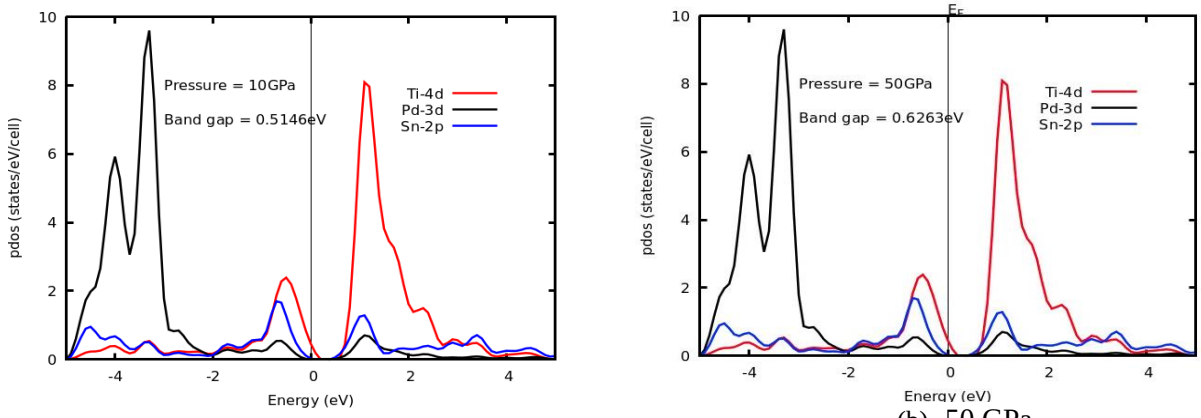

(a) 10 GPa (b) 50 GPa

Figure 5 (a-b): The PDOS of TiPdSn

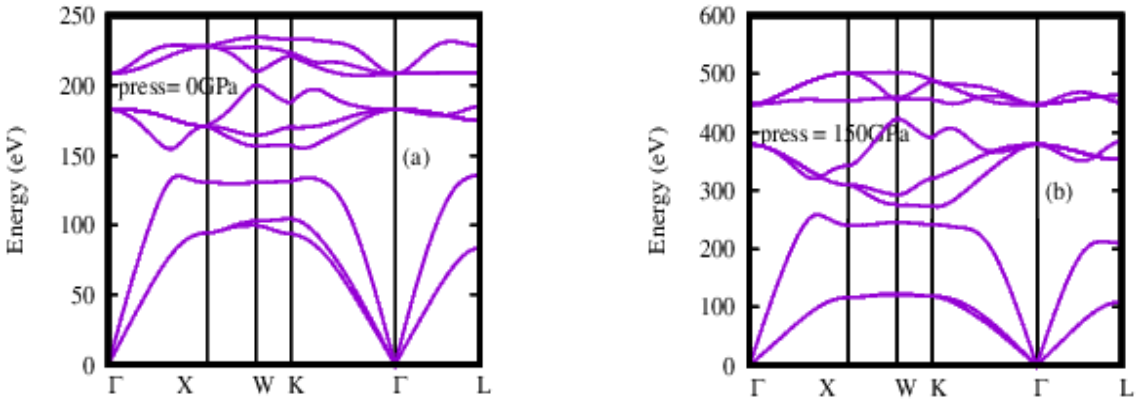

Figure 6(a-b): Phonon dispersion curves along symmetry of TiPdSn at pressures (0 GPa and 150 GPa)

Optical Properties

In order to ascertain half-Heusler (HH) of TiPdSn for optoelectronic uses, optical characteristics are vital. The criterion related to optical properties of TiPdSn is discussed in this section. The optical property is plotted against energy in Electron-Volts (eV) and is displayed in Figures 7(a-h).

The optical properties are linked to the dielectric functions $\varepsilon(\omega) = \varepsilon_1(\omega) + i\varepsilon_2(\omega)$Where $\varepsilon(\omega)$ is the number of information regarding the interaction of incoming radiation with matter. $\varepsilon_1(\omega)$ and $\varepsilon_2(\omega)$ are real and imaginary dielectric functions.

Optical properties such as optical conductivity, extinction, energy loss, absorption, reflectivity and refractive index are determined from the real and imaginary dielectric function (Gautier *et al*., 2015).

Fig 7: Optical properties of TiPdSn in cubic phase. (a) Real dielectric, (b) Imaginary dielectric function, (c) Refractive index and (d) Absorption coefficient.

Fig. 7a illustrates the real dielectric function of TiPdSn at the pressure of 0GPa and 150GPa. It is seen that the static dielectric constant $\varepsilon_1(0)$ is 19.42 and 24.59 for 0GPa and 150GPa respectively, which is in good agreement with literature (Babalola *et al*., 2019).

Fig. 7b illustrates the imaginary dielectric function having its highest peak at 2.63 eV (150 GPa) and 1.57 eV (0 GPa), which occurs within the visible-light-region of the spectrum. The various Peaks represent the different Inter-bandTransitions from the Valence-band to the Conduction-band. Fig. 7c depicts the refractive indices of TiPdSn. Here, the static refractive index is at 4.30 (150 GPa) and 5.11 (0 GPa) respectively. Fig. 7d shows the Absorption Coefficient, which notifies, how Light is absorbed by a Material. It is seen that the Absorption Coefficient increases steadily with increasing Photon-Energy. The sharp increase in the graph indicates that TiPdSn absorbs plenty of light, which allows Electrons to be excited to the Conduction-Band-Region.

Fig.7 f shows the Extinction Coefficient of TiPdSn, which increases with increasing Photon-Energy. It reaches a maximum peak at 1.78 eV (0GPa) and 2.59 eV (150GPa), with other peaks appearing, as the Photon-Energy increases, before steadily decreasing. Energy is lost during inelastic scattering of electrons with light, and this is illustrated in Figures. 7 g from 12 eV to 20 eV for 150 GPa and 13 eV to 13 eV for 0 GPa: The energy loss is the effect of electron-excitation.

The optical conductivity of TiPdSn is illustrated in fig.7 h, with a lot of peaks appearing within the energy range considered, with the highest peak appearing at 2.64 eV (150 GPa) and 1.78 eV (0 GPa).

The Reflectivity is shown in Fig.7e, indicating the highest peak at 6.10 eV (150GPa) and 5.8 eV (0GPa), also revealing its maximum reflectivity of 61 % (150GPa) and 58 % (0GPa).

From all Indications, TiPdSn Half-Heusler-Alloys indicates an indirect band-gap-semiconductor. The mechanical properties indicate that the Half-Heusler-Alloys are ductile, with increase in pressure leading to an increase in elastic constants and moduli. The mechanical stability of TiPdSn is achieved. The optical properties Half-Heusler of TiPdSn indicates its Application in the Opto-electronic-Industries.

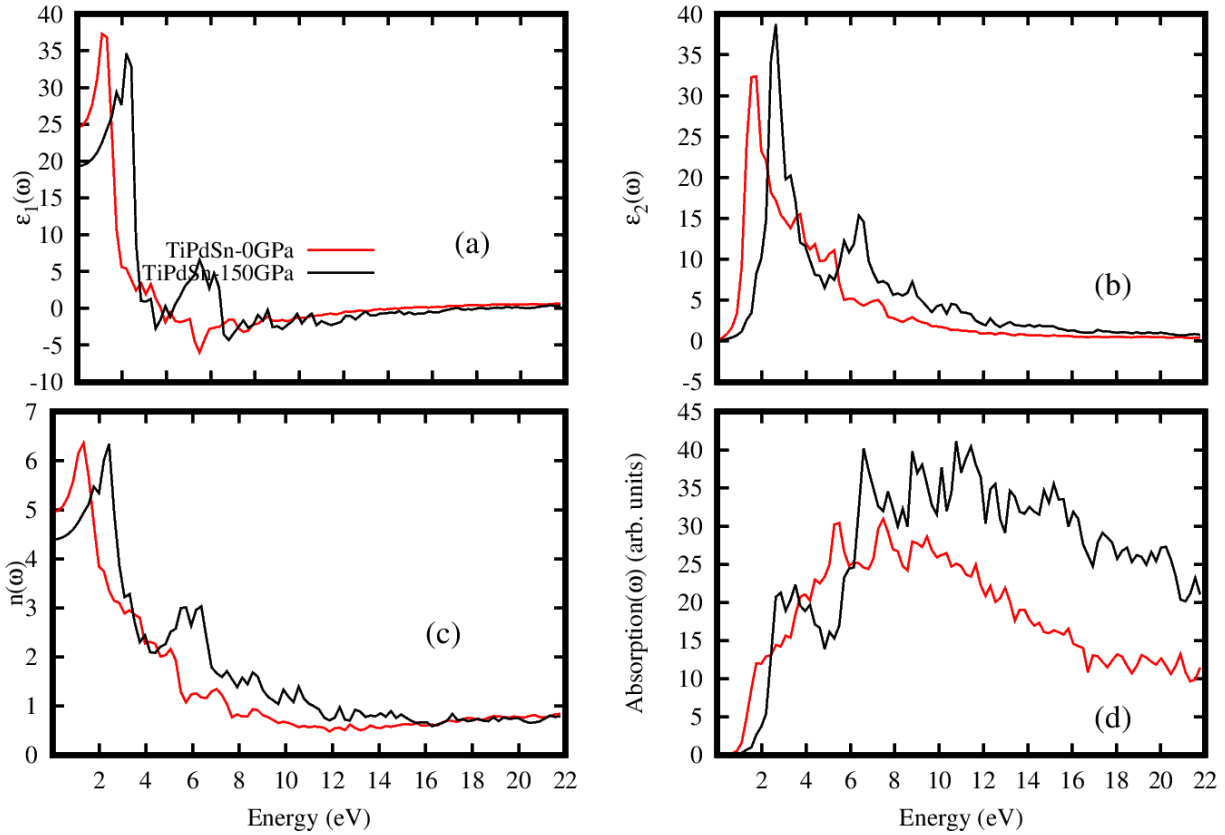

Figure 7(a-d): Optical properties of TiPdSn: (a) real dielectric function (b) imaginary dielectric function (c) refractivity and (d) absorption coefficient

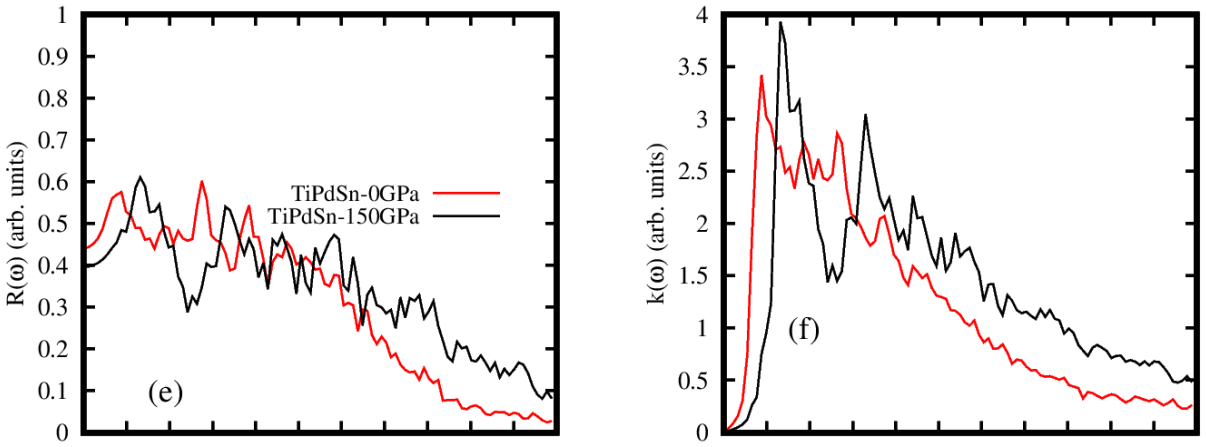

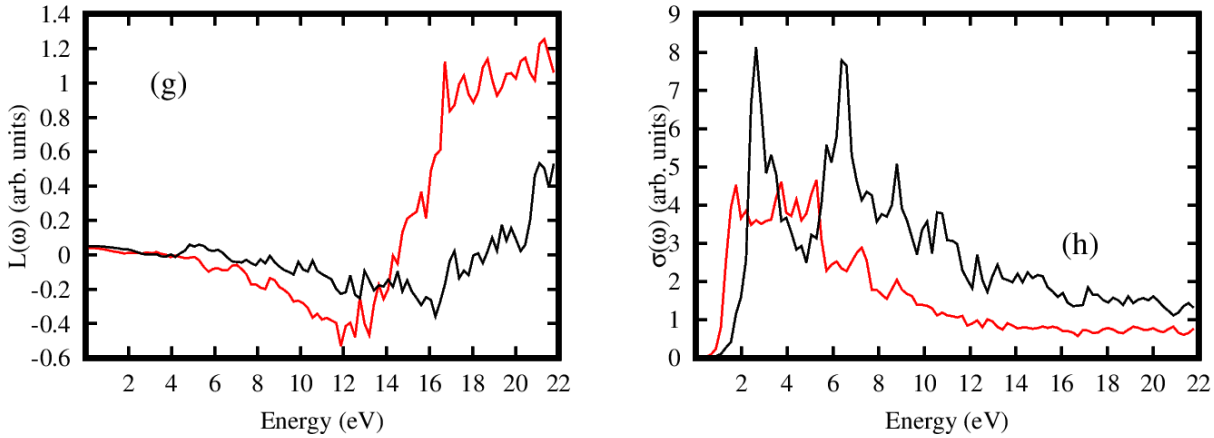

Figure 7(e-h): Optical properties of TiPdSn: (e) reflectivity (f) extinction coefficient (g) energy loss and (h) optical conductivity

CONCLUSION

In conclusion, physical properties of TiPdSn have been examined from first-principles computation at zero and at rising pressures. TiPdSn was shown to be an indirect band gap semiconductor. The mechanical property exhibit that the HH alloy is ductile, with the elastic constants rising with increasing pressure, also with the moduli increasing with increasing pressure and that the mechanical stability was obtained. In the spin-electronic industries, the optical properties of TiPdSn half-Heusler alloy application are of importance.

REFERENCES

Aigbekaen, E.E., and Ighrakpata, F. C. (2022). The First Principal Study Of The Structural, Electronic, Elastic, Vibrational And Thermal Properties Of Cscl Type-Ercu Alloy. *AAN Journal of Sciences, Engineering & Technology Vol. 1, Issue 1, pp. 1-11.*

Aigbekaen, E.E., Okei, J., and Ighrakpata, F.C. (2023). First-Principles Study: Some Physical Properties of Half-Heusler Alloys XCrBi (X=Hf, Ti, and Zr). *Journal of Science and Technology Research 5(4), 118-127.*

Babalola, M.I. and Iyorzor, B.E. (2021). Electronic, mechanical, vibrational and optical properties of TalrX (X= Ge and Sn): a DFT approach. *Molecular Physics, p.e1995062.*

Babalola, M.I. and Iyorzor, B.E. (2019). A search for half metallicity in half Heusler alloys. *Journal of Magnetism and Magnetic Materials, 491, p.165560.*

Babalola, M.I., Iyorzor, B.E., and Okocha, O.G. (2019). Origin of half-metallicity in XCrBi (X=Hf, Ti, and Zr) half-Heusler alloys. *Materials Research Express, 6(12), p.126301.*

Babalola,M I., Omamoke, O.E, and Enaroseha. (2023). Pressure induced structural phase transition and influence of pressure on the electronic and mechanical properties of TiPdSn: an ab initio study. *Iranian Journal of Physics Research. Vol. 23, No.3.*

Canfield, P.C., Thompson, J.D., Beyermann, W.P., Lacerda, A., Hundley, M.F., Peterson, E., Fisk, Z. and Ott, H.R. (1991). Magnetism and heavy fermion- Like behavior in the RBiPt series. *Journal of applied physics, 70(10), pp.5800-5802.*

Chadov, S., Q, X., Kübler, J., Fecher, G.H., Felser, C. and Zhang, S.C. (2010). Tunable multifunctional topological insulators in ternary Heusler compounds. *Nature materials, 9(7), pp.541-545.*

Dal Corso, A. (2016). "Elastic constants of beryllium: a first-principles investigation." *Journal of Physics: Condensed Matter 28, no. 7: 075401.*

Damewood, L., Busemeyer, B., Shaughnessy, M., Fong, C.Y., Yang, L.H. and Felser, C. (2015). Stabilizing and increasing the magnetic moment of half- metals: The role of Li in halfHeuslerLiMn Z N, P, Si). *Physical Review B, 91 (6), p.064409.*

Gautier, R., Zhang, X., Hu, L., Yu, L., Lin, Y., Sunde, T.O., Chon, D., Poeppelmeier, K.R. and Zunger, A. (2015). Prediction and accelerated laboratory discovery of previously unknown 18-electron ABX compounds. *Nature chemistry, 7(4), pp.308-316.*

Gautier, R., Zhang, X., Hu, L., Yu, L., Lin, Y., Sunde, T.O., Chon, D., Poeppelmeier, R.R. and Zunger, A. (2015). Prediction and accelerated laboratory discovery of previously unknown 18-electron ABX compounds. *Nature chemistry, 7(4), pp.308-316.*

Giannozzi, P., Andreussi, O., Brumme, T., Bunau, O. , Nardelli, M.B., Calandra, M. , Car, R., cavazzoni, C., Ceresoli, D., Cococcioni, M., and Colonna, N. (2017). Advanced capabilities for materials modelling with Quantum ESPRESSO. *Journal of physics: Condensed matter, 29(46), p.465901.*

Goll, G., Marz, M., Hamann, A., Tomanic, T., Grube, K., Yoshino, T. and Takabatake, T. (2008).Thermodynamic and transport properties of the non-centrosymmetric superconductor LaBiPt. *Physica B: Condensed Matter, 403(5-9), pp.1065-1067.*

Gu, J.B., Wang, C.J., Cheng, Y., Zhang, L., Cai, L.C., and Ji, G.F. (2015). Structural, elastic, thermodynamic, electronic properties and phase transition in half-Heusler alloy NiVSb at high pressures. *Computational Materials Science, 96, pp.72-80.*

Inomata, K., Okamura, S., Goto, R. and Tezuka, N. (2003). Large tunneling magnetoresistance at room temperature using a Heusler alloy with the B2 structure. *Japanese journal of applied physics, 42(4B), p.L419.*

Iyorzor, B. E., Babalola.M.I., and Aigbekaen,E.E. (2018). Ab initio Calculation of the Structural, Mechanical and Thermodynamic Properties of Beryllium Sulphides,BeS,. *J.Appl.Sci.Environ.Manage.,Vol.22(1), 41-46.*

Iyorzor,B.E., Babalola.M.I.,and Aigbekaen,E.E. (2018). Ab initio Calculation of the Structural, Mechanical and Thermodynamic Properties of Beryllium Sulphides, BeS.. *J.Appl.Sci.Environ.Manage.,Vol.22(1), 41-46.*

Kaur, K. (2017). TiPdSn: A half Heusler compound with thermoelectric performance. *EPL (Europhysics Letters), 117(4), p.47002.*

Khandy S.A., and Gupta, D.C. (2017). DFT investigations on mechanical stability , electronic structure and magnetism in Co2TaZ (Z=Al, Ga, In) Heusler alloys. *Semicond. Sci. Technol. 32 (12)*. https://doi.org/10.1088/1361-6641/aa9785.

Khandy, S.A., and Chai, J.D., (2021). Strain engineering of electronic structure, phonon, and thermoelectric properties of p-type half-Heusler semiconductor. *Journal ofAlloys and Compounds, 850, p. 156615*.

Khenata,R. A., Bouhemadou, M. Hichour, H. Baltache, D., Rached, M. (2006). Elastic and optical properties of BeS, BeSe and BeTe under pressure, *Solid State Electron. 50 (2006) 1382–1388*, https://doi.org/10.1016/j.sse.2006.06.019.

Kocak, B. and Ciftci, Y.O. (2018). The effect of pressure on structural, electronic, elastic, vibration and optical properties of ScXSb (X= Ni, Pd, Pt) compounds. *Computational Condensed Matter, 14, pp.176-185*.

Noda, Y. , Shimada, M., and Koizumi, M. (1979). Synthesis of high-pressure phases of vanadium-cobalt-antimony (VCoSb) and vanadium-iron-antimony (VFeSb) with a dinickelindium (Ni21n)(B82) type structure. *Inorganic Chemistry, 18(11), pp.3244-3246.*

Okunzuwa, I. S. and Aigbekaen, E.E. (2021). Structural Optimization, Electronic Band Structure, Mechanical and Thermodynamics Properties of Fe3 Al. *Physical Science International (JournalArticle no.PSIJ.67620) 25(2): 1-11*.

Oogane, M., Sakuraba, Y., Nakata, J., Kubota, H., Ando, Y., Sakuma, A. and Miyazaki, T. (2006). Large tunnel magnetoresistance in magnetic tunnel junctions using $C0_2MnX$ (X= Al, Si) Heusler alloys. Journal of Physics D: *Applied Physics, 39(5), p.834.*

Sarker, S., Rahman, M.A., and Khatun, R. (2021). Study of structural, elastic, electronics, optical and thermodynamic properties of Hf2PbC under pressure by ab-initio method. *Computational Condensed Matter, 26, p.e00512.*

Van Engen, P.G., Buschow, K .J., Jongebreur, R., anclErman, M. (1983). PtMnSb, a material with very high magneto-optical Kerr effect. *Applied Physics Letters, 42(2), pp.202-204.*

Webster, P.J., Ziebeck, K.R.A., Town, S.L., and Peak, M.S. (1984). Magnetic order and phase transformation in Ni2MnGa. *Philosophical Magazine B, 49(3), pp.295-310.*

Zheng, W., Lu, Y., Li, Y., Wang, J., Hou, Z., and Shao, X. (2020). Structural and thermoelectric properties of Zr-doped TiPdSn half-Heusler compound by first-principles calculations. *Chemical Physics Letters, 741, p.137055.*

Zilber, T., Cohen, S., Fuks, D. and Gelbstein, Y. (2019). TiNiSn half-Heusler crystals grown from metallic flux for thermoelectric applications. *Journal of Alloys and Compounds, 781, pp.1132-1138.*